Spectroscopy 21 (2007) 151–160
IOS Press

The effect of diabetes mellitus on rat skeletal extensor digitorum longus muscle tissue: An FTIR study

Ozlem Bozkurt [a], Mehmet Dincer Bilgin [b] and Feride Severcan [a,*]

[a] *Department of Biology, Middle East Technical University, 06531, Ankara, Turkey*
[b] *Department of Biophysics, Faculty of Medicine, Adnan Menderes University, Aydin, Turkey*

Abstract. Diabetes mellitus (DM) is a chronic disorder of carbohydrate, fat and protein metabolism, which is characterized by a defective insulin secretory response. Skeletal muscle takes role in determination of carbohydrate and lipid metabolism, therefore; it is one of the target tissues of diabetes. Herein this study, application of Fourier Transform Infrared (FTIR) spectroscopy in diabetic skeletal Extensor Digitorum Longus (EDL) muscle tissues will be presented which highlight the promise of this technique in medical research. Type I DM was induced in rats by injection of streptozotocin (STZ) which is one of the most popular experimental models. In diabetes, a significant increase was observed in lipid order together with an increase in hydration of phospholipid molecules in membrane structure. There was a decrease in lipid and nucleic acid content in diabetic EDL muscles. A dramatic increase in the bandwidth of amide II band (1540 cm^{-1}) and shifting of the position of this band to lower frequency values in diabetes was observed indicating structural changes occurring in proteins of diabetic EDL muscles.

Keywords: Diabetes mellitus, skeletal muscle, EDL, FTIR

1. Introduction

Diabetes mellitus (DM) is a destructive disease gaining more importance as it affects a large number of people of all social conditions throughout the world. DM is a chronic disorder of carbohydrate, fat and protein metabolism with a defective or deficient insulin secretory response, which in turn results an impaired carbohydrate use by the tissues. This property of DM causes some metabolic disturbances which lead to chronic, irreversible damage to vital organs and systems [1]. Apart from its role in aiding the uptake of glucose to tissues, insulin regulates a variety of other metabolic responses, including facilitating entry of amino acids into cells for the production of cellular proteins, increasing precursors for nucleic acid synthesis, transporting critical cellular ions as well as controlling the expression of a number of genes associated with carbohydrate and fatty acid metabolism [1,2].

Skeletal muscle, being one of the major tissues determining carbohydrate and lipid metabolism in the body, is affected from the lack of insulin action which is seen in diabetic conditions [3]. It is composed of different fiber types having different levels of metabolic enzymes and contractile proteins [4]. The classification of muscle fiber types is as type I fibers (slow-contracting, red, oxidative) and type II fibers

* Corresponding author: Feride Severcan, Department of Biology, Middle East Technical University, 06531, Ankara, Turkey. Tel.: +90 312 210 51 66; Fax: +90 312 210 79 76; E-mail: feride@metu.edu.tr

(fast-contracting, white), which are further divided into type IIa (fast-contracting oxidative-glycolytic) and type IIb (fast-contracting glycolytic) fibers [5,6].

There have been controversial results reported in literature concerning the effect of diabetes on the protein, lipid content and the breakdown or synthesis metabolisms of macromolecules of different skeletal muscle fiber types [7–10]. In this current study, Fourier Transform Infrared (FTIR) spectroscopy was used to obtain detailed structural information about the effects of type I DM on the macromolecular composition of Extensor Digitorum Longus (EDL) skeletal muscle tissues. FTIR spectroscopy is a non-destructive, valuable technique due to its high sensitivity in detecting the changes in the functional groups belonging to biological tissue components, simultaneously [11–15]. The technique is especially useful for the analysis of secondary structural characterization of proteins.

2. Materials and methods

2.1. Materials

Streptozotocin (STZ) was purchased from Sigma (Sigma Chemical Company, Saint Louis, Missouri, USA) and potassium bromide (KBr) was obtained from Merck (Merck Company, Darmstadt, Germany). All chemicals were obtained from commercial sources at the highest grade of purity available.

2.2. Animals

Approval of the study was obtained from the Ethics Committee of Adnan Menderes University. Adult male Wistar rats (Experimental Animal Center, Adnan Menderes University, Aydin) weighing 250–300 g were selected randomly. The rats were fed with a Standard diet with water ad libitum, and kept in conventional room with controlled light (12:12, dark:light), temperature ($22 \pm 1^{\circ}$C), relative humidity (40–50%) and ventilation (15 air changes per hour).

The rats were separated into two groups as control ($n = 5$) and diabetic ($n = 6$). Control rats received a single dose of citrate buffer (0.05 mol/l, pH 4.5) injection, intraperitoneally. Induction of diabetes was made by an intraperitonal injection of single dose of streptozotocin (STZ) (50 mg/kg) dissolved in 0.05 mol/l citrate buffer (pH 4.5). 5% dextrose solution was given to the diabetic group rats to prevent the mortality due to hypoglycemic shock that can take place in the first 6 hours after STZ administration. 3 days after the STZ administration, blood glucose levels were measured using a glucometer (One Touch Horizon Blood Glucose Monitoring System/Glucometer, USA). The ones having a blood glucose level higher than 300 mg/dl were accepted as diabetic. After 6 weeks, the rats were decapitated and their EDL muscles were dissected and stored at -80°C until use.

2.3. Sample preparation for FTIR studies

The muscle fiber samples were dried in a LABCONCO freeze drier (FreeZone®, Model 77520) overnight in order to remove the water content. The dried samples were ground with liquid nitrogen in a liquid nitrogen-cooled colloid mill (Retsch MM200) to obtain tissue powder. The tissue powder was mixed with dried potassium bromide (KBr) in a mortar (at a ratio of 0.5:150) and dried in the freeze drier for 18 hours to remove all traces of remaining water. The mixture was compressed into a thin KBr disk under a pressure of $\sim$100 kg/cm^2 for in an evacuated die producing transparent disk for the use in FTIR spectrometer.

Infrared spectra were obtained using a Perkin–Elmer Spectrum One FTIR spectrometer (Perkin–Elmer Inc., Boston, MA, USA) equipped with a MIR TGS detector. The interfering spectrum of air and KBr transparent disk was recorded as background and substracted automatically by using appropriate software (SpectrumOne software).

2.4. Infrared spectroscopy

Collection of spectra and all data manipulations were carried out using SpectrumOne software (Perkin–Elmer). The spectra of muscle samples were recorded at room temperature in the 4000–400 cm^{-1} frequency region. Each interferogram was collected with 50 scans at 4 cm^{-1} resolution. Each sample was scanned as three different pellets under the same conditions, all of which gave identical spectra. The average spectra of these three replicates were used in detailed data and statistical analysis. Using the same software the spectra were first smoothed with nineteen-point Savitsky–Golay smooth function to remove the noise. After the averages of three replicates of the same samples were taken, the spectra were baseline corrected and were normalized with respect to specific bands for visual demonstration. In determination of the mean values for the peak positions, band area and the bandwidth values, the spectra belonging to each individual of the groups was considered and in detailed analysis spectra that are not normalized were used. The band positions were measured using the frequency corresponding to the center of weight. Band areas were calculated from smoothed and baseline corrected spectra using SpectrumOne software. The bandwidth values of specific bands were calculated as the width at 0.75 $\times$ height of the signal in terms of cm^{-1}.

2.5. Statistics

The results were expressed as 'mean $\pm$ standard deviation (SD)'. The differences in means were analyzed statistically using non-parametric Mann–Whitney U test. A p value less than or equal to 0.05 was considered as statistically significant. The degree of significance was denoted as $p < 0.05^{*}$, $p < 0.01^{**}$, $p < 0.001^{***}$.

3. Results and discussion

The effects of diabetes on skeletal muscle tissues gained attention in the early 1960s. Although the effects of DM on skeletal muscles have been documented previously by some biochemical and physiological studies [11,12,16,17], it is very important to describe the effects of the disease on the composition, structure, and function of macromolecules in skeletal muscle tissues. This current study is conducted to determine the biochemical and biophysical changes occurring in EDL skeletal muscle tissue as a result of Type I DM at molecular level using FTIR spectroscopy. EDL muscle is largely composed of Type II skeletal muscle fibers (3% type I, 57% type IIa, 40% type IIb) having a fast-contracting glycolytic characteristic [6,18].

Figure 1 shows the representative infrared spectra of control EDL muscle in 4000–400 cm^{-1} region. The main bands were labelled in the figure and detailed band assignments are given in Table 1. As seen from the figure, the FTIR spectrum of EDL muscle is a complex spectrum and is composed of several bands originating from functional groups of different macromolecules; such as lipids, proteins, carbohydrates and nucleic acids. Therefore, for more detailed information spectral analysis were performed in three distinct regions, namely 3650–3000 cm^{-1}, 3025–2800 cm^{-1} and 2000–400 cm^{-1}.

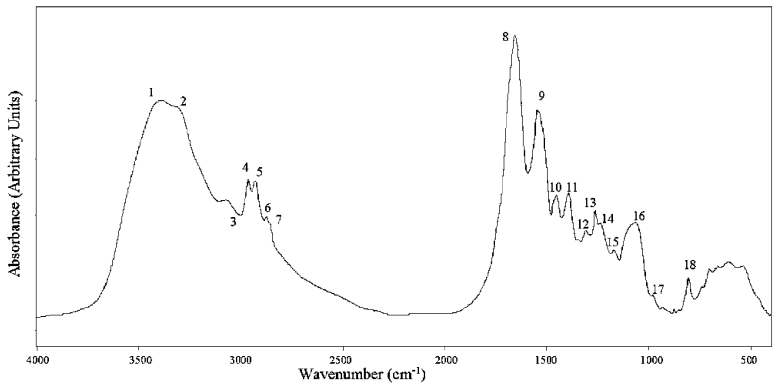

Fig. 1. The representive infrared spectra of control EDL muscle in 4000–400 cm^{-1} region. The spectra were normalized with respect to the amide A band.

Table 1

General band assignment of FTIR spectrum of skeletal muscle tissue based on literature [11,12,15,14,19–22]

Peak No.	Wavenumber (cm^{-1})	Definition of the spectral assignment
1	3400	O–H stretching (Amide A), hydrogen-bonded intermolecular OH groups of proteins and glycogen
2	3307	Mainly N–H stretching (Amide A) of proteins with the little contribution from O–H stretching of polysaccharides and intermolecular H bonding
3	3014	Olefinic=CH stretching vibration: unsaturated lipids, cholesterol esters
4	2962	CH_3 asymmetric stretching: mainly lipids, with the little contribution from proteins, carbohydrates, nucleic acids
5	2929	CH_2 asymmetric stretching: mainly lipids, with the little contribution from proteins, carbohydrates, nucleic acids
6	2874	CH_3 symmetric stretching: mainly proteins, with the little contribution from lipids, carbohydrates, nucleic acids
7	2855	CH_2 symmetric stretching: mainly lipids, with the little contribution from proteins, carbohydrates, nucleic acids
8	1656	Amide I (protein C=O stretching)
9	1540	Amide II (protein N–H bend, C–N stretch)
10	1452	CH_2 bending: mainly lipids, with the little contribution from proteins
11	1392	COO^- symmetric stretching: fatty acids
12	1343	Amide III vibrations of collagen
13	1261	PO_2^- asymmetric stretching, non-hydrogen-bonded: mainly nucleic acids with the little contribution from phospholipids
14	1236	PO_2^- asymmetric stretching, fully hydrogen-bonded: mainly nucleic acids with the little contribution from phospholipids
15	1170	CO–O–C asymmetric stretching: glycogen and nucleic acids
16	1080	PO_2^- symmetric stretching: nucleic acids and phospholipids C–O stretch: glycogen, polysaccharides, glycolipids
17	976	$C–N^+–C$ stretch: nucleic acids, ribose-phosphate main chain vibrations of RNA
18	802	Vibrations in N-type sugars in nucleic acid backbone

Figure 2A–C shows the representative infrared spectra of control and diabetic EDL muscles in the 3650–3000 cm^{-1}, 3025–2800 cm^{-1} (C–H stretching region) and 2000–400 cm^{-1} (fingerprint region),

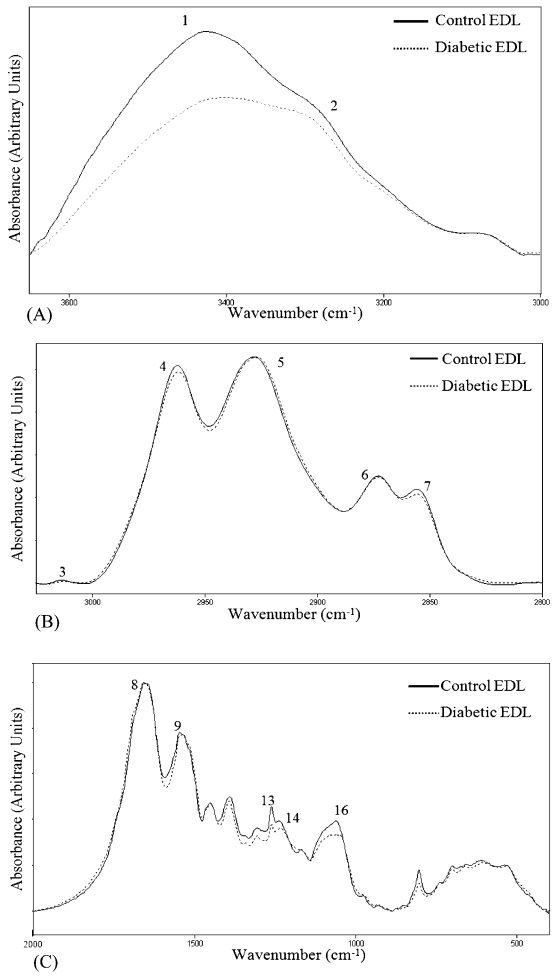

Fig. 2. The representative infrared spectra of control and diabetic EDL muscles in: (A) 3650–3030 cm^{-1} region, (B) 3025–2800 (C–H stretching region), and (C) 2000–400 cm^{-1} region (finger print region) The spectra were normalized with respect to the CH_2 asymmetric stretching band ((A) and (B)) and to the amide I band (C).

respectively. The spectra were normalized with respect to the CH_2 asymmetric stretching band (for 3650–3000 and 3025–2800 cm^{-1} regions) and to the amide I band (for fingerprint region). The numerical comparisons of the changes in the means of the frequencies and the area values of the main bands for control and diabetic EDL muscles were listed in Table 2.

In the C–H region, absorptions arising from the C–H stretching vibrations of olefinic =CH, CH_2 and CH_3 groups are monitored. The CH_2 antisymmetric and symmetric stretching and the CH_3 asymmetric stretching bands originate from the lipid acyl chains, whereas the CH_3 symmetric stretching bands are mainly due to proteins (Table 1). The intensity and/or more accurately the area of the infrared absorption bands arising from a particular molecule is directly proportional to the concentration of that molecule. As seen from Fig. 2B and Table 2, there was a decrease ($p < 0.05^{*}$) in the areas of the CH_3 asymmetric and the CH_2 symmetric stretching bands suggesting a decrease in the lipid content of the diabetic EDL muscle [23].

Table 2
Changes in the frequency and area values of the infrared bands for control and diabetic EDL muscles

Band No	Band frequency (cm^{-1})		Band area	
	Control EDL ($n = 5$)	Diabetic EDL ($n = 6$)	Control EDL ($n = 5$)	Diabetic EDL ($n = 6$)
2	3399.43 ± 23.62	$3385.79 \pm 25.30 \downarrow$	49.18 ± 9.50	$36.76 \pm 8.51 \downarrow$
3	3015.38 ± 3.64	$3014.25 \pm 0.93 \downarrow$	1.18 ± 0.28	$0.93 \pm 0.27 \downarrow$
4	2962.52 ± 0.41	$2962.70 \pm 0.43 \uparrow$	3.71 ± 0.68	$2.60 \pm 0.64^{*} \downarrow$
5	2929.23 ± 0.54	$2927.77 \pm 0.81^{**} \downarrow$	4.07 ± 1.00	$3.18 \pm 0.88 \downarrow$
6	2873.78 ± 0.46	$2874.58 \pm 0.75 \uparrow$	1.30 ± 0.30	$1.00 \pm 0.27 \downarrow$
7	2854.95 ± 0.09	$2855.70 \pm 0.38^{**} \uparrow$	1.12 ± 0.25	$0.77 \pm 0.18^{*} \downarrow$
8	1655.75 ± 1.05	$1656.7 \pm 4.68 \uparrow$	16.79 ± 5.73	$12.05 \pm 4.16 \downarrow$
9	1540.04 ± 0.45	$1536.02 \pm 4.87^{*} \downarrow$	11.04 ± 3.73	$7.66 \pm 2.66 \downarrow$
10	1453.13 ± 1.10	$1454.76 \pm 3.06 \uparrow$	3.33 ± 0.87	$2.88 \pm 0.86 \downarrow$
11	1392.56 ± 1.02	$1393.23 \pm 2.65 \uparrow$	4.59 ± 1.23	$3.35 \pm 1.01 \downarrow$
12	1343.92 ± 0.59	$1343.05 \pm 2.62 \downarrow$	0.96 ± 0.25	$0.82 \pm 0.24 \downarrow$
13	1261.18 ± 0.42	$1261.55 \pm 0.30 \uparrow$	1.77 ± 0.44	$1.45 \pm 0.39 \downarrow$
14	1236.52 ± 1.80	$1233.88 \pm 1.19^{*} \downarrow$	3.06 ± 0.82	$2.35 \pm 0.69 \downarrow$
15	1169.98 ± 0.45	$1169.99 \pm 2.04 \uparrow$	1.51 ± 0.39	$1.18 \pm 0.30 \downarrow$
16	1068.03 ± 5.03	$1066.82 \pm 4.91 \downarrow$	6.16 ± 0.75	$5.12 \pm 0.56^{*} \downarrow$
17	978.19 ± 2.03	$981.12 \pm 1.72 \downarrow$	0.30 ± 0.07	0.30 ± 0.05
18	802.98 ± 0.11	$803.22 \pm 0.30 \uparrow$	0.56 ± 0.07	$0.53 \pm 0.09 \downarrow$

The values are the mean $\pm$ SD for each group. Comparisons were done by Mann–Whitney U-test. Downward arrow indicates a decrease and upward arrow indicates an increase with respect to the control.

*The degree of significance was denoted as: $p < 0.05$.

**The degree of significance was denoted as: $p < 0.01$.

The shifts in the frequencies of the CH_2 stretching vibrations can be used as a marker for the detection of changes in lipid order [24–26]. In our study the frequency of the CH_2 asymmetric stretching band shifted to lower values (from 2929.23 ± 0.54 cm^{-1} to 2927.77 ± 0.81 $cm^{-1}, p < 0.01^{**}$) in diabetic group of EDL muscle. This shifting demonstrates an increase in the order of the system together with an increase in the number of trans conformers of lipid molecules, which further results in a more rigid membrane structure. One possible explanation for the observed membrane rigidity can be the free radical formation resulting from the lipid peroxidation seen in DM, which modifies the lipid composition of the membranes. In many studies concerning oxidative stress, a decrease in the membrane unsaturated/saturated fatty acid ratio was detected along with the formation of cross-linked lipid–lipid and lipid–protein moieties [26–28]. Therefore, the altered unsaturated/saturated fatty acid ratio of membrane phospholipids evidently results with the increase in rigidity of membrane.

Amide I band can be used for the determination of protein secondary structure as the frequency of vibrations of this band is sensitive to protein conformation [21,22,29]. The results of this study indicate a very slight shift to lower values observed in the frequency of amide I band in diabetic group of EDL muscle (Table 2). In addition, amide II band originating from proteins in the system also gives information about protein secondary structure. As it can be seen from Table 2 and Fig. 2C, there was an easily observed shift to lower values in the frequency of amide II band from 1540 cm^{-1} to 1536 cm^{-1} ($p < 0.05^{*}$) in diabetic group. The Amide II band around 1544 cm^{-1} is assigned to α-helix structures of proteins [12]. The shift to lower frequency values, as in our case, indicate a change in protein secondary structure and conformation, probably by an increase in content of random coil structures [30]. Apart

Table 3
Changes in some of the bandwidth values and area ratios of the infrared bands for control and diabetic EDL muscles

Functional group	Control EDL ($n = 5$)	Diabetic EDL ($n = 6$)
Bandwidth of amide II	28.10 ± 0.70	$34.80 \pm 4.6^{**} \uparrow$
Ratio of areas of CH_2 asym. strech. + CH_2 Sym. strech./CH_3 sym. strech.	4.19 ± 0.07	$4.00 \pm 0.05^{**} \downarrow$

The values are the mean ± SD for each group. Comparisons were done by Mann–Whitney U-test. Downward arrow indicates a decrease and upward arrow indicates an increase with respect to the control.

*The degree of significance was denoted as: $p < 0.05$.

**The degree of significance was denoted as: $p < 0.01$.

from the frequency changes, the changes in bandwidth values of protein bands may provide information about protein conformation in the system as the amide bands result from the superimposition of some subbands corresponding to the different types of secondary structure of proteins [31]. There was an increase in the bandwidth of amide II band from 28.10 ± 0.70 to 34.80 ± 4.6 ($p < 0.01^{**}$) for diabetic EDL muscle, supporting that the protein secondary structure is altered in diabetic conditions (Table 3).

One of the important factors affecting the membrane structure and dynamics is the amount of proteins and lipids in the membranes [32]. A precise lipid-to-protein ratio can be derived from the FTIR spectrum by calculating the ratio of the areas of the bands arising from lipids and proteins. In Table 3, changes in the lipid-to-protein ratio calculated as the ratio of the sum of the areas of the CH_2 asymmetric and symmetric stretching bands to the area of the CH_3 symmetric stretching band was demonstrated. This ratio was lower in diabetic EDL muscle ($p < 0.01^{**}$). The decrease of this ratio in diabetic EDL muscle suggests that there was a much pronounced decrease in lipid content when compared to the decrease in protein content in diabetic conditions.

The shoulder of the Amide A band located at approximately 3420 cm^{-1} is assigned to hydrogen-bonded intermolecular the OH groups, and the shoulder at 3307 cm^{-1} is assigned to the N–H stretching mode [12,33,34]. As it can be seen from Fig. 2A, the decrease in the shoulder at 3420 cm^{-1} in diabetic group can be explained by the reduced contribution from glycogen OH absorbtion [12,14].

Both lipid and carbohydrate fuels can be utilized by healthy skeletal muscle and its fuel selection can rapidly change upon the stimulus and energy demands. The loss of flexibility of skeletal muscle to switch between lipid and carbohydrate fuels is shown to be an important aspect of insulin resistance seen in type II diabetes and obesity [17]. Baldwin et al. (1973) [35] showed that type I fibers exhibit a greater reliance on lipid at resting conditions and during moderate exercise, whereas type II fibers rely on carbohydrate fuel for energy generation. The results of this study are in accordance with these studies in showing the changes occurred in the content of these macromolecules in diabetic conditions.

In the 1300–1000 cm^{-1} spectral range of the FTIR spectrum the bands originating from the stretching modes of the P=O bond present in the phosphate moieties (PO_2^-) of phospholipids and nucleic acids can be observed [36,37]. These bands can be used to monitor the changes in the hydration state of the head group of phospholipids in the polar–nonpolar interface of membranous structures and alterations in the quantity, conformational state, and the degree and position of phosphorylation of the nucleic acids in DNA and RNA [38,39]. As reported in the literature, the frequency of the PO_2 asymmetric stretching mode is at 1240–1260 cm^{-1} indicating completely non-hydrogen-bonded PO_2^- groups, and approximately at 1220 cm^{-1} indicating free phosphate groups [19,20]. It can be seen from Fig. 2C and Table 2 that, the frequency of the band located at 1236 cm^{-1} shifts to a lower value ($p < 0.05^{*}$) for diabetic EDL muscle indicating an increase in hydrogen bonding of phospholipid head groups and

nucleic acids. The increase in hydration can occur by binding of the phospholipids molecules either with the oxygen of the phosphate head group or with its aqueous environment [40]. Moreover, there is a slight shift to lower values in the PO_2 symmetric stretching band located at 1068 cm^{-1} in diabetic EDL muscle. These shifts to lower values in the frequencies of these bands in diabetes seem to support the ordering effect of diabetes on membrane structure mentioned earlier. As seen in Table 2 the area of the PO_2 symmetric stretching band located at 1080 cm^{-1} decreased in diabetic group ($p < 0.05^*$) indicating a decrease in the content of nucleic acids and phospholipids in the membrane structures of EDL muscles.

In the present study the effect of Type I DM on fast-contracting EDL muscle tissue was investigated using FTIR spectroscopy. FTIR spectroscopy is an excellent nondestructive and time consuming technique for the investigation of biological systems due to its high sensitivity and ability to give valuable information, which might have diagnostic use in biological systems. Owing to these properties of the technique, it can easily be used to detect disease-induced changes.

In conclusion, the results of the current study shows an increase in lipid order together with the increase in hydration of phospholipids molecules in membrane structure, a decrease in lipid and nucleic acid content and a change in protein secondary structure in diabetic EDL muscles. Moreover, this study is first to report the changes in membrane structures and protein conformation of skeletal muscle tissue in diabetic conditions. As the usage of FTIR as a diagnostic tool is currently gaining importance, the present study is further important as it sheds light on the structural alterations occurring in the macromolecular content of diabetic skeletal muscle giving valuable information for clinical studies and differentiation of diabetic tissues from healthy ones at molecular level.

Acknowledgement

This work was supported by METU Research Fund BAP-2006-R-07-02-17.

References

[1] S.R. Stapleton, Selenium: An insulin-mimetic, *Cellul. Molec. Life Sci.* **57** (2000), 1874–1879.
[2] R.M. O'Brien and D.K. Granner, Regulation of gene expression by insulin, *Physiol. Rev.* **76** (1996), 1109–1161.
[3] R.A. DeFronzo, E. Jacot, E. Jequier, E. Maeder, J. Wahren and J.P. Felber, The effect of insulin on the disposal of intravenous glucose, *Diabetes* **30** (1981), 1000–1007.
[4] P. Nemeth and D. Pette, Succinate dehydrogenase activity in fibres classified by myosin ATPase in three hind limb muscles of rat, *J. Physiol. (London)* **320** (1981), 73–80.
[5] W.K. Engel, The essentiality of histo- and cytochemical studies of skeletal muscle in the investigation of neuromuscular disease, *Neurology (Minneapolis)* **12** (1962), 778–794.
[6] M.D. Delp and C. Duan, Composition and size of type I, IIA, IID/X, and IIB fibers and citrate synthase activity of rat muscle, *J. Appl. Physiol.* **80**(1) (1996), 261–270.
[7] R.B. Armstrong and C.D. Ianuzzo, Compensatory hypertrophy of skeletal muscle fibers in streptozotocin-diabetic rats, *Cell Tiss. Res.* **181** (1977), 255–266.
[8] J.F. Hopp and W.K. Palmer, Effect of glucose and insulin on triacylglycerol metabolism in isolated normal and diabetic skeletal muscle, *Metabolism* **40**(3) (1991), 223–225.
[9] J. He, S. Watkins and D.E. Kelley, Skeletal muscle lipid content and oxidative enzyme activity in relation to muscle fiber type in type 2 diabetes and obesity, *Diabetes* **50** (2001), 817–823.
[10] E. Bernroider, A. Brehm, M. Krssak, C. Anderwald, Z. Trajanoski, G. Cline, G.I. Shulman and M. Roden, The role of intramyocellular lipids during hypoglycemia in patients with intensively treated type 1 diabetes, *J. Clin. Endocrinol. Metab.* **90** (2005), 5559–5565.
[11] H. Takahashi, S.M. French and P.T.T. Wong, Alterations in hepatic lipids and proteins by chronic ethanol intake: A high-pressure Fourier transform Infrared spectroscopic study on alcoholic liver disease in the rat alcohol, *Clin. Exp. Res.* **15**(2) (1991), 219–223.

[12] A. Melin, A. Perromat and G. Deleris, Pharmacologic application of Fourier transform IR spectroscopy: In vivo toxicity of carbon tetrachloride on rat liver, *Biopolymers (Biospectroscopy)* **57** (2000), 160–168.
[13] K.Z. Liu, R. Bose and H.H. Mantsch, Infrared spectroscopic study of diabetic platelets, *Vibrational Spectroscopy* **28** (2002), 131–136.
[14] G. Cakmak, I. Togan and F. Severcan, 17 β-Estradiol induced compositional, structural and functional changes in rainbow trout liver, revealed by FT-IR spectroscopy: A comparative study with nonylphenol, *Aquatic Toxicology* **77** (2006), 53–63.
[15] N. Toyran, P. Lasch, D. Naumann, B. Turan and F. Severcan, Early alterations in myocardia and vessels of the diabetic rat heart: An FTIR microspectroscopic study, *Biochem. J.* **397**(3) (2006), 427–436.
[16] P. Malenfant, D.R. Joanisse, R. Theriault, B.H. Goodpaster, D.E. Kelley and J.-A. Simoneau, Fat content in individual muscle fibers of lean and obese subjects, *International Journal of Obesity* **25** (2001), 1316–1321.
[17] B.H. Goodpaster and D. Wolf, Skeletal muscle lipid accumulation in obesity, insulin resistance, and type 2 diabetes, *Pediatric Diabetes* **5** (2004), 219–226.
[18] M.A. Ariano, R.B. Armstrong and V.R. Edgerton, Hindlimb muscle fiber populations of five animals, *J. Histochem.* **21** (1973), 51–55.
[19] B. Rigas, S. Morgellot, I.S. Goldman and P.T.T. Wong, Human colorectal cancers display abnormal Fourier-transform infrared spectra, *Proc. Natl. Acad. Sci.* **87** (1990), 8140–8144.
[20] P.T.T. Wong, R.K. Wong, T.A. Caputo, T.A. Godwin and B. Rigas, Infrared spectroscopy of exfoliated human cervical cells: Evidence of extensive structural changes during carcinogenesis, *Proc. Natl. Acad. Sci.* **88** (1991), 10988–10992.
[21] M. Jackson, B. Ramjiawan, M. Hewko and H.H. Mantsch, Infrared microscopic functional group mapping and spectral clustering analysis of hypercholosterolomic rabbit liver, *Cell. Mol. Biol.* **44**(1) (1998), 89–98.
[22] D.J. Lyman and J. Murray-Wijelath, Vascular graft healing: I. FTIR analysis of a implant model for studying the healing of a vascular graft, *J. Biomed. Mater. Res. (Appl. Biomater.)* **48** (1999), 172–186.
[23] N. Toyran, F. Zorlu, G. Dönmez, K. Öğe and F. Severcan, Chronic hypoperfusion alters the content and structure of proteins and lipids of rat brain homogenates: A Fourier transform infrared spectroscopy study, *Eur. Biophys. J.* **33** (2004), 549–554.
[24] H.H. Mantsch, Biological application of Fourier Transform Infrared Spectroscopy: A study of phase transitions in biomembranes, *J. Mol. Structure* **113** (1984), 201–212.
[25] F. Severcan, Vitamin E decreases the order of the phospholipid model membranes in the gel phase: An FTIR study, *Bioscience Reports* **17** (1997), 231–235.
[26] M.T. Curtis, D. Gilfor and J.L. Farber, Lipid peroxidation increases the molecular order of microsomal membranes, *Arch. Biochem. Biophys.* **235** (1984), 644–649.
[27] G. Levin, U. Cogan, Y. Levy and S. Mokady, Riboflavin deficiency and the function and fluidity of rat erythrocyte membranes, *J. Nutr.* **120** (1990), 857–861.
[28] T.G. Niranjan and T.P. Krishnakantha, Membrane changes in rat erythrocyte ghosts on ghee feeding, *Mol. Cell. Biochem.* **204** (2000), 57–63.
[29] P.I. Haris and F. Severcan, FTIR spectroscopic characterization of protein structure in aqueous and non-aqueous media, *J. Molecular Catalysis B: Enzymatic* **7** (1999), 207–221.
[30] K. Kugo, M. Okuno, K. Kitayama, T. Kitaura, J. Nishino, N. Ikuta, E. Nishio and M. Iwatsuki, Fourier transform IR attenuated total reflectance study on the secondary structure of poly (γ-methyl L-glutamate) surfaces treated with formic acid, *Biopolymers* **32** (1992), 197–207.
[31] F. Dousseau and M. Pezolet, Determination of the secondary structure content of proteins in aqueous solutions from their amide I and amide II infrared bands. Comparison between classical and partial least-squares methods?, *Biochemistry* **29** (1990), 8771–8779.
[32] B. Szalontai, Y. Nishiyama, Z. Gombos and N. Murata, Membrane dynamics as seen by Fourier Transform Infrared Spectroscopy in a cyanobacterium, synechocystis PCC 6803. The effects of lipid unsaturation and the protein-to-lipid ratio, *Biochim. Biophys. Acta* **1509** (2000), 409–419.
[33] S. Raudenkolb, W. Hübner, W. Rettig, S. Wartewig and R.H.H. Neubert, Polymorphism of ceramide 3. Part 1: an investigation focused on the head group of N octadecanoylphytosphingosine, *Chem. Phys. Lipids* **123** (2003), 9–17.
[34] A. Nilsson, A. Holmgren and G. Lindblom, Fourier-transform infrared spectroscopy study of dioleoylphosphatidylcholine and monooleoylglycerol in lamellar and cubic liquid crystals, *Biochemistry* **30** (1991), 2126–2133.
[35] K.M. Baldwin, J.S. Reitman, R.L. Terjung, W.W. Winder and J.O. Holloszy, Substrate depletion in different types of muscle and liver during prolonged running, *Am. J. Physiol.* **225** (1973), 1045–1050.
[36] M. Diem, S. Boydston-White and L. Chiriboga, Infrared spectroscopy of cells and tissues: shining light onto a novel subject, *Applied Spectroscopy* **53** (1999), 148A–161A.
[37] J. Liquier and E. Taillandier, Infrared spectroscopy of nucleic acids, in: *Infrared Spectroscopy of Biomolecules*, Wiley, USA, 1996, pp. 131–158.
[38] R. Mendelsohn and H.H. Mantsch, Fourier transform infrared studies of lipid-protein interaction, in: *Progress in Protein-Lipid Interactions,* Vol. 2, Elsevier Science Publishers, the Netherlands, 1986, pp. 103–147.

[39] G.I. Dovbeshko, N.Y. Gridina, E.B. Kruglova and O.P. Pashchuk, FTIR spectroscopy studies of nucleic acid damage, *Talanta* **53** (2000), 233–246.
[40] C.R. Flach, J.W. Brauner and R. Mendelson, Calcium ion interactions with insoluble phospholipid monolayer films at the A/W interface: External reflection-absorption infrared studies, *Biophys J*. **65**(5) (1993), 1994–2001.